Mon. Not. R. Astron. Soc. **390,** L78–L82 (2008) doi:10.1111/j.1745-3933.2008.00542.x

Puzzling X-rays from the new colliding wind binary Wolf–Rayet 65 (WC9d)

L. M. Oskinova⋆ and W.-R. Hamann
Potsdam University, Universitätsstandort Golm, Haus 28, Potsdam 14476, Germany

Accepted 2008 July 29. Received 2008 July 25; in original form 2008 July 7

ABSTRACT

We report the discovery of variability in the X-ray emission from the Wolf–Rayet type star WR 65. Using archival *Chandra* data spanning over 5 yr, we detect changes of the X-ray flux by a factor of 3 accompanied by changes in the X-ray spectra. We believe that this X-ray emission originates from wind–wind collision in a massive binary system. The observed changes can be explained by the variations in the emission measure of the hot plasma, and in the different absorption column along the binary orbit. The X-ray spectra of WR 65 display prominent emission features at wavelengths corresponding to the lines of strongly ionized Fe, Ca, Ar, S, Si and Mg. WR 65 is a carbon-rich WC9d star that is a persistent dust maker. This is the first investigation of any X-ray spectrum for a star of this spectral type. There are indications that the dust and the complex geometry of the colliding wind region are pivotal in explaining the X-ray properties of WR 65.

Key words: stars: early-type – stars: individual: WR 65 – stars: Wolf–Rayet – X-rays: stars.

1 INTRODUCTION

More than 54 per cent of all Wolf–Rayet (WR) stars are in binary systems that consist of a WR and an OB-type star (Wallace 2007). The collision between two stellar winds in these systems produces characteristic signatures in different wavelength bands that can include non-thermal radio emission (Eichler & Usov 1993), copious and variable X-rays (Stevens, Blondin & Pollock 1992), and dust emission in the infrared (IR) (Williams, van der Hucht & Thé 1987).

Subject of this *Letter* is the WC9d star WR 65. Williams et al. (1987) reported the presence of warm dust in this object. They discussed that in early-type WC stars an increase in the wind density provided by, for example, shock compression in colliding winds in binary systems may be sufficient to result in grain formation. Zubko (1998) found no need to invoke binarity to explain the presence of dust in late WC stars. He fitted the observed IR spectrum of WR 65 assuming a single star with stellar mass loss in the form of dust with $\dot{M}_{\rm d} = 5.4 \times 10^{-10}\,{\rm M}_{\odot}\,{\rm yr}^{-1}$ and surrounded by a dust shell with an inner radius of $520\,R_{*}$. Leitherer, Chapman & Koribalski (1997) detected radio emission from WR 65, but could not constrain its spectral index.

In a previous paper (Oskinova et al. 2003), we demonstrated that single WC-type stars are X-ray quiet and proposed that all X-ray active WC stars must be in binary systems. X-ray emission from WR 65 was detected and tentatively explained as a result of wind–wind collision. In this Letter, we report on the X-ray light curve of WR 65 and changes in its X-ray spectra that unambiguously confirm its status as a colliding-wind binary (CWB).

⋆E-mail: lida@astro.physik.uni-potsdam.de

2 WR 65 AND ITS X-RAY LIGHT CURVE

The coordinates of WR 65 from different sources are compiled in Table 1. The coordinates from SIMBAD and the USNO-B1.0 catalogue agree well with the source location in the *Chandra* HRI-I image. Except for WR 65, there are no other known objects at this position. WR 65 is a probable member of the cluster Pismis 20, which contains one more WR star, WR 67, and has a distance of $d = 3272 \pm 303$ pc (Turner 1996).

We fit the optical spectrum of WR 65 and its available photometry using the Potsdam Wolf–Rayet (PoWR) stellar atmosphere models (Hamann & Gräfener 2003). The deduced stellar parameters are listed in Table 2.

A wind-blown bubble with a radius of 7 arcmin is known around WR 65 (Marston 1997). Giacani & Dubner (2004) discovered a H I shell with a radius of 22 pc surrounding WR 65 and WR 67. The infrared *Spitzer* IRAC image of WR 65 at 8 μm is shown in Fig. 1. Despite its unfavourable location close to the edge of the detector, a rather compact nebula around WR 65 is visible. The radius of the nebula is ≈1.5 arcmin or 1.4 pc. Given the strong mass-loss rate of WR 65 and its strong ultraviolet field, it is plausible that the nebula is physically associated with this star.

In the X-ray sky, WR 65 is located in a very interesting neighbourhood (see Fig. 2). The star is 7.4 arcmin away from the supernova remnant (SNR) G320.4−1.2 and 4 arcmin away from the X-ray bright 'Cir Pulsar' and its associated pulsar wind nebula (PWN). The SNR and the Cir pulsar are at the distance $d = 5.2 \pm 1.4$ kpc (Gaensler et al. 2002). This region of the sky is often observed, and serendipitous X-ray observations of WR 65 are in archives.

The most homogeneous data set found in archives are from *Chandra* ACIS-I observations conducted from year 2000 to 2005.

© 2008 The Authors. Journal compilation © 2008 RAS

Table 1. Coordinates of WR 65 from different sources.

Reference	Band	RA J2000	Dec. J2000
SIMBAD	optical	$15^{h}\,13^{m}\,41\overset{s}{.}68$	$-59^{\circ}\,11'\,43\overset{''}{.}3$
Chapman et al. (1999)	radio	$15^{h}\,13^{m}\,41\overset{s}{.}49$	$-59^{\circ}\,11'\,43\overset{''}{.}8$
Chandra HRI-I	X-ray	$15^{h}\,13^{m}\,41\overset{s}{.}76$	$-59^{\circ}\,11'\,44\overset{''}{.}1$
Catalogue USNO-B1.0	optical	$15^{h}\,13^{m}\,41\overset{s}{.}73$	$-59^{\circ}\,11'\,43\overset{''}{.}4$

Table 2. Stellar parameters of WR 65 (from Hamann et al., in preparation).

E_{B-V}	$\log L_{bol}/L_{\odot}$[a]	υ_{∞} (km s^{-1})	$\dot{M}$ ($M_{\odot}$ yr^{-1})[b]
2.4	5.8,. . .,6.4	≈2000	$10^{-4.6}, \ldots, 10^{-4.1}$

[a]Depending on the adopted reddening law.
[b]Assuming a clumping contrast $D = 10$.

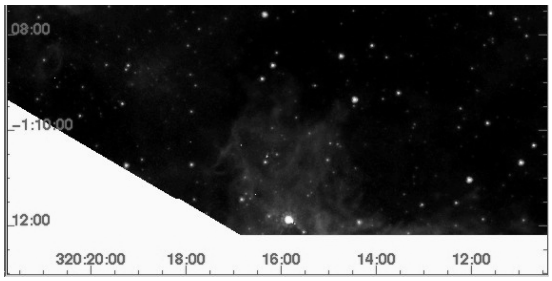

Figure 1. Archival *Spitzer* image (8 μm). WR 65 is the bright object at the bottom, close to the detector edge. The coordinates are galactic.

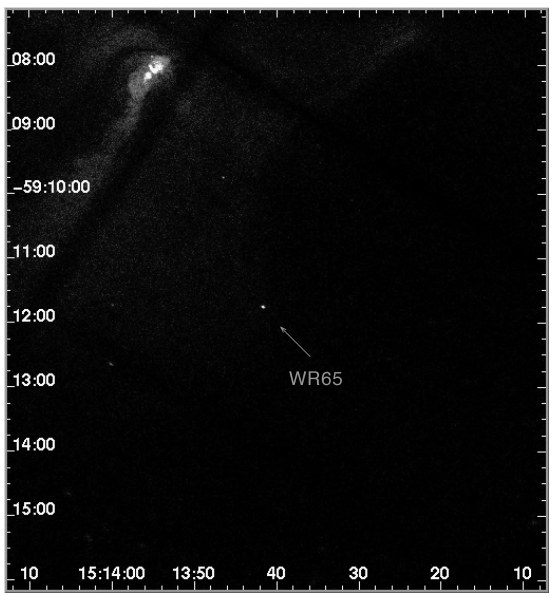

Figure 2. Archival *Chandra* ACIS-I image (0.2–12.0 keV) of WR 65. The observation is from 2005 October 18. The bright object in the upper left-hand corner of the image is the pulsar PSR B1509−58. WR 65 is projected on to the outskirts of the pulsar wind emission. The coordinates are equatorial (J2000). North up, east left.

In 2005, WR 65 was also observed on one occasion by *Chandra* HRI-I and twice by *XMM–Newton*, but was not detected during *XMM–Newton* observations affected by high-radiative background.

The local X-ray background is high because WR 65 is projected on the peripheral region of the PWN mentioned above. Therefore,

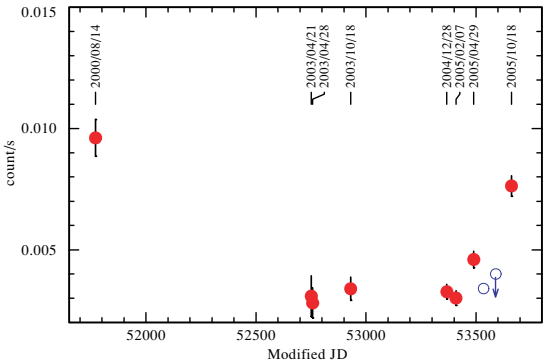

Figure 3. X-ray (0.4–10.0 keV) light curve of WR 65. The red dots show *Chandra* ACIS-I count rates. The blue dots show count rates converted to ACIS-I rates from *Chandra* HRC-I and *XMM–Newton* MOS (upper limit).

we paid special attention to the background subtraction. Conveniently, the X-ray emission from the PWN is well studied (Gaensler et al. 2002; Yatsu et al. 2005). DeLaney et al. (2006) find that it is constant over at least 12 yr. We defined background regions as annuli around a stellar point source.

Fig. 3 shows the background-subtracted X-ray light curve of WR 65 that displays a surprisingly high level of variability. Such strong X-ray variability in massive stars is observed only in binary systems (Oskinova, Clarke & Pollock 2001; Corcoran et al. 2005). The WR 65 X-ray light curve gives strong evidence that the star is a CWB. Unfortunately, the light curve is too sparse to search for the period. Given the time interval between the two recorded maxima, one may conclude that the period is not longer than about 5 yr.

3 WR 65: X-RAY SPECTRAL VARIABILITY

Five of the *Chandra* observations of WR 65 yielded enough counts for a crude X-ray spectral analysis. The background-subtracted spectra obtained at different epochs are displayed in Fig. 4. The spectral energy distribution is harder than for single WR stars (Ignace, Oskinova & Brown 2003). The unresolved emission features coincide with the location of lines of Fe, Ca, Ar, S, Si and Mg (cf. Figs 4 and 5) in collisionally ionized X-ray spectra. Interestingly, the iron lines at ≈6.7 keV (1.8 Å) are weaker at some epochs compared to others (e.g. they seem to disappear completely on 2005 February 07). If real, this may reflect the change of the temperature in the hot plasma.

The X-ray spectrum of WR 65 in high states displays strong emission features in the 2–4 Å range (see top panel in Fig. 4). Weak lines of Ca XIX (λ 3.2 Å), Ca XX (λ 3.0 Å) and Ar XVIII (λ 3.7 Å) are sometimes observed in the X-ray spectra of CWBs, e.g. the WC8 binary γ^2 Vel (Schild et al. 2004), the WN6 binary WR 25 (Raassen et al. 2003) and the LBV binary η Car (Hamaguchi et al. 2007). It seems plausible to assume that the unresolved Ca and Ar lines contribute to the emission 'bump' at 2–4 Å in the WR 65 spectrum. However, the strength of this emission complex in WR 65 is much higher than observed in any other CWB. We rule out its origin from the background PWN emission, because there are no emission features at 2–4 Å in the spectra extracted from an annulus region around WR 65.

In CWBs consisting of an OB star and a WC star, the latter has a significantly denser, C, O-enriched wind that is basically opaque for X-rays (Oskinova et al. 2003). When in the course of the orbital motion, the wind collision region (WCR) is at superior conjunction

© 2008 The Authors. Journal compilation © 2008 RAS, MNRAS **390,** L78–L82

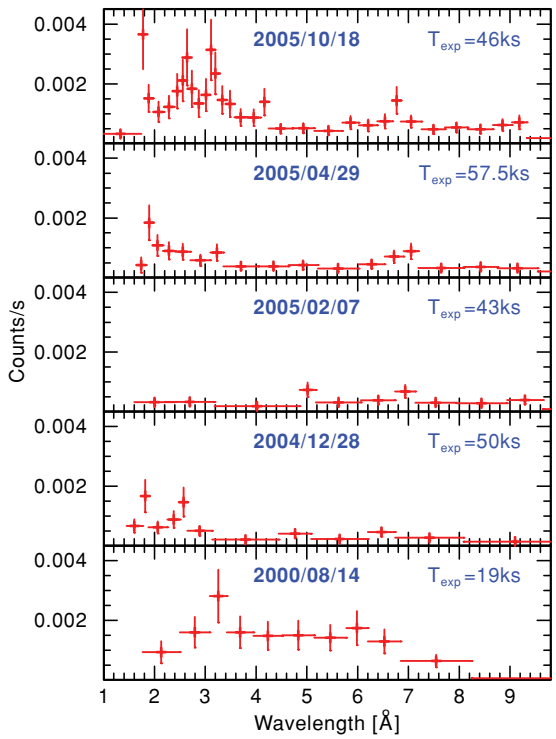

Figure 4. *Chandra* ACIS-I background-subtracted spectra of WR 65 at different epochs. The date of the observation and the exposure time is given in each panel.

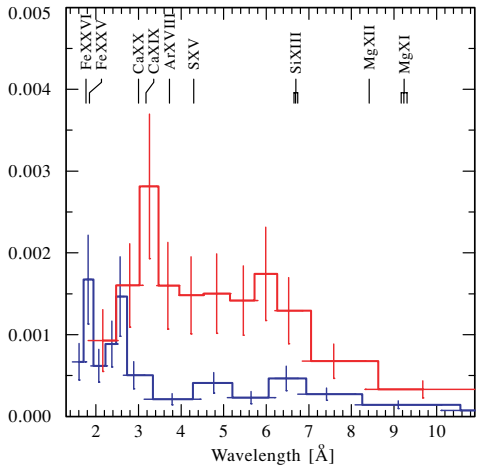

Figure 5. *Chandra* ACIS-I spectra of WR 65 in high (red lines) and low (blue lines) states (obtained on 2000 August 14 and 2004 December 28, respectively). Wavelengths of strong spectral lines are indicated.

relative to the WC star (with respect to the observer), the X-rays generated in the WCR suffer strong absorption. Despite many still unclear details, this general picture is observationally confirmed by the X-ray spectral analysis of the WC + O type binaries WR 140 and γ^2 Vel. In these systems, the strongest photo-attenuation is seen in low X-ray states, while the lowest photo-attenuation is found when the X-ray flux is high (Rauw et al. 2000; Schild et al. 2004; Pollock et al. 2005).

To investigate how X-ray spectral variations are coupled with the variation of the absorption column, we fit a model to the observed spectra and check how the model parameters vary between the different epochs.

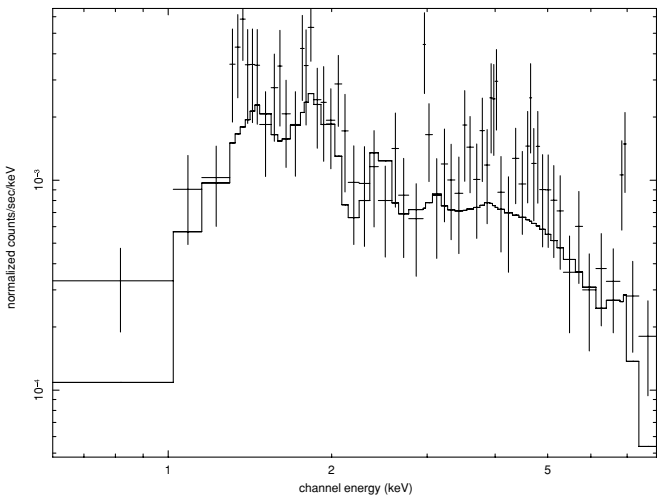

Figure 6. ACIS-I spectrum of WR 65 obtained on 2005 October 18 and the best-fitting spectral model – $tbabs(N_{\rm H,1}) * apec(kT_1) + tbabs(N_{\rm H,2}) * apec(kT_2)$. The XSPEC spectral fitting package was used. For the model parameters, see the text.

Zhekov (2007) found that only models with non-equilibrium ionization can reproduce the *detailed* X-ray spectra of CWBs. However, he noted that these spectra can be crudely described by thermal plasma emission with some 'average' temperature. Using the XSPEC software (Arnaud 1996), we tried to fit the observed WR 65 spectra alternatively with non-equilibrium ionization, PSHOCK and power-law models. However, no meaningful constraints on model parameters could be obtained because of the poor quality of the spectra. Finally, we select a two-temperature thermal plasma model (APEC, Smith et al. 2001) where each component is allowed to suffer different degrees of attenuation – the '2T2$N_{\rm H}$' model. This model provides a first insight into the properties of the system by constraining the model parameters. We refer to the plasma with lower temperature kT_1 as the 'soft' model component, and to the plasma with higher temperature kT_2 as the 'hard' model component. As demonstrated in Figs 6 and 7, the 2T2$N_{\rm H}$ model sufficiently well reproduces the shape of the WR 65 spectra observed at different epochs.

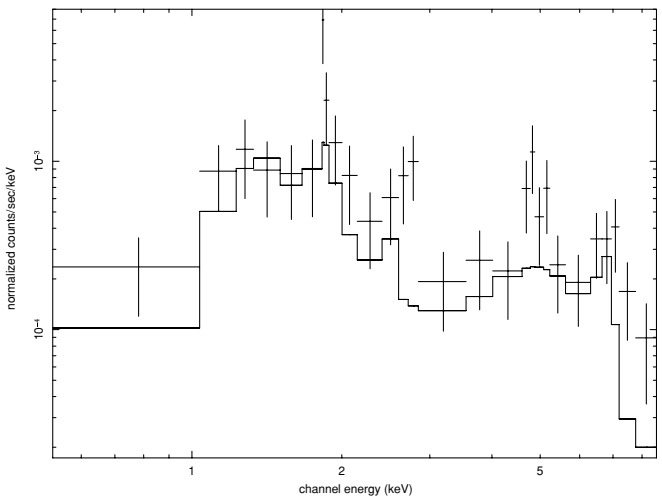

Figure 7. Same as in Fig. 6 for the spectrum obtained on 2004 December 28.

We assume solar composition. Selecting WC-wind abundances results in scaling down of the parameter that describes normalization of the emission measure (EM), but the effect of abundances on *spectral shape* cannot be discriminated given the poor quality of available data.

The spectrum of WR 65 with highest signal-to-noise ratio and its best-fitting model is shown in Fig. 6. The temperatures inferred from spectral fitting are $kT_1 = 1.0 \pm 0.2$ keV and $kT_2 = 13.4 \pm 7.3$ keV. Such temperatures can be expected from the collision of metal-enriched winds in wide binaries. The temperature is highest at the point of head-on collision, and is decreasing along the shock cone (Stevens et al. 1992).

The interstellar absorption column density towards the Cir pulsar, $N_{\rm H,ism} = 1 \times 10^{22}$ cm^{-2}, is well constrained and consistent with the color excess inferred from our fitting of the WR 65 spectral energy distribution. The neutral hydrogen column densities are $N_{\rm H,1} = (2.3 \pm 0.3) \times 10^{22}$ cm^{-2} for the soft component and $N_{\rm H,2} = (12.2 \pm 4.1) \times 10^{22}$ cm^{-2} for the hard component. The column density to the soft component, $N_{\rm H,1}$, exceeds the interstellar column by a factor of more than 2, but it is lower than the column density to the hard component, $N_{\rm H,2}$. This indicates that the hotter plasma is more deeply embedded.

From the spectrum obtained at 2005 October 18, the model flux is $F_{\rm X}(0.6\text{–}9.0\,{\rm keV}) = 1.2 \times 10^{-13}$ erg s^{-1} cm^{-2}, which corresponds to $L_{\rm X} = 1.1 \times 10^{32}$ erg s^{-1}, or in terms of stellar bolometric luminosity to $\log L_{\rm X}/L_{\rm bol} = -7.2, \ldots, -7.8$. The flux of the soft spectral component, $F_{\rm X}(0.6\text{–}2.0\,{\rm keV}) = 8.3 \times 10^{-15}$ erg s^{-1} cm^{-2}, corresponds to $L_{\rm X}(0.6 - 2.0\,{\rm keV}) = 1.0 \times 10^{31}$ erg s^{-1} which is similar to the X-ray luminosity of a single O dwarf (Oskinova 2005).

Spectra observed at other epochs were also fitted with the 2T2$N_{\rm H}$ model. For illustration, the spectrum obtained in the low state and its corresponding best-fitting model is shown in Fig. 7. Fig. 8 shows the model parameters depending on the time of observation. Within the errorbars, the temperatures kT_1 and kT_2, and the absorption column to the source for the soft component, $N_{\rm H,1}$ are similar at all observed epochs, and therefore are not plotted in Fig. 8. In contrast, the column density to the hard component, $N_{\rm H,2}$, changes at different epochs (panel A of Fig. 8). Variations in the EM of the hard and soft components are shown in panels B and C of Fig. 8. The EM of the soft component changes strongly, reflecting the X-ray light-curve variations, while the changes in the EM of the hard component are less pronounced.

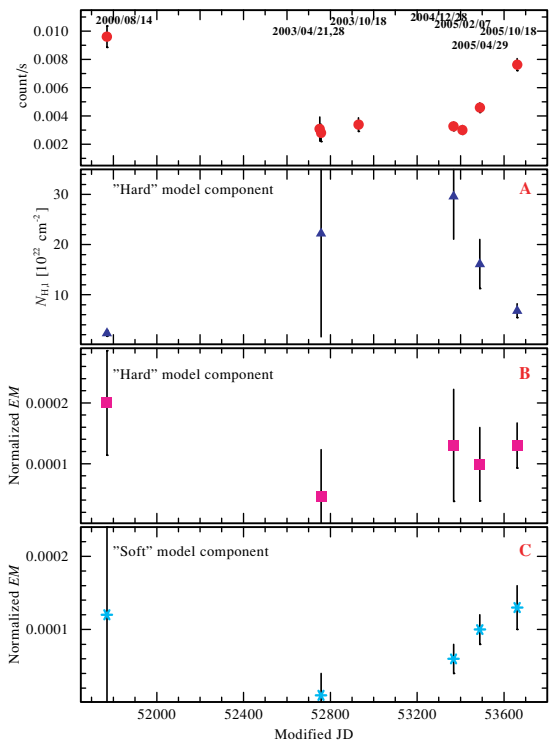

Figure 8. Upper panel: same as in Fig. 3. Panel A: variations of absorption column density of the hard component obtained from spectral fits. Panel B: normalization factor that characterizes the emission measure of the hard component. Panel C: normalization factor of the soft component.

4 DISCUSSION

The main findings from the analysis of WR 65 X-ray spectra obtained at different epochs are (i) the spectra display emission features at the wavelengths of the lines of strongly ionized Fe, Ca, Ar, S, Si and Mg; (ii) the star shows strong spectral X-ray variability; (iii) the spectra can be fitted with a two-temperature model, consisting of a soft component with $0.3 \lesssim kT_1 \lesssim 1.5$ keV and a hard component with $2 \lesssim kT_2 \lesssim 20$ keV; (iv) the absorption for the hard component is strong and variable, while the absorption for the soft component is less severe and nearly constant and (v) the changes in the EM are stronger for the soft component.

Can these observations be explained in the framework of a colliding wind model? Corcoran et al. (2005) compare the 2.0–10.0 keV light curves of WR 140 and η Car (both are systems with high eccentricity and high inclination) and note that they are very similar. Pittard et al. (1998) explain the light curve (2.0–10.0 keV) of η Car using a hydrodynamic simulation of colliding winds. They show that the data are broadly consistent with the X-ray emission being moderately low throughout most of the orbit. However, a sharp peak occurs near periastron, when a greater fraction of the stellar winds collides and the higher pre-shock densities and the lower pre-shock velocities result in stronger radiative cooling. The eclipse occurs immediately after periastron passage when the companion of η Car swings behind the LBV star with its dense wind.

It is hard to see how a similar model can be used to explain the X-ray variability of WR 65. Strong variations in the absorbing column indicate that the orbit of WR 65 has a high inclination too. Considering the light curve (Fig. 3), we can rule out that WR 65 has a period of a few days: the two data points obtained in 2003 April indicate constant count rates over at least a week. Moreover, two data points in the light curve separated by two months (2004 December and 2005 February) are similar, while there is an increase in emission by nearly 70 per cent in the next two months. Therefore, WR 65 has most likely an orbital period of a few years. In this case, the long duration of the minimum is inconsistent with its interpretation as attenuation by the wind of the WC star immediately after periastron passage. Quite different from the short-duration rise of column density observed in WR 140 and η Car, the column density in WR 65 is persistently very high, $N_{\rm H,2} \gtrsim 10^{23}$ cm^{-2}, sharply decreasing only at the maximum X-ray light.

The temporary variations of column density in WR 65 are similar to those measured in the WC8 + O binary γ^2 Vel (Rauw et al. 2000). Its hard X-ray emission increases by a factor of $\sim$4 when column density decreases by factor of approximately few during the passage of weak-wind inner side of the shock cone across the line of sight (Willis, Schild & Stevens 1995; Rauw et al. 2000; Schild et al. 2004).

In WR 65, the soft X-ray emission is present at all observed epochs. Its variation can be explained by changing emission

© 2008 The Authors. Journal compilation © 2008 RAS, MNRAS **390,** L78–L82

measure, while the absorption is nearly constant and comparably low. A soft spectral component in the low state is also observed in γ^2 Vel, V444 Cyg and η Car. The origin of soft X-rays in these stars is attributed either to individual stellar winds or to a circumstellar nebula. Accordingly, in these objects, the absorbing column to the soft component is similar to the interstellar absorbing column. In contrast, we find for WR 65 that $N_{\rm H,ism} < N_{\rm H,1} < N_{\rm H,2}$, and the EM of the soft component changes with the X-ray light curve. Thus, it is unlikely that the intrinsic wind emission of a companion is solely responsible for the soft X-rays from WR 65.

WR 65 is a persistent dust maker (van der Hucht 2001). Monnier et al. (2002) note that binary stars that are persistent dust makers have nearly circular orbits. We can assume that the same holds for WR 65. There is a growing number of WC9d binary stars that constitute the 'pinwheel' class of objects (Marchenko & Moffat 2007; Tuthill et al. 2008). In these binary systems, the dust is formed in the wind collision region and is distributed along a wide (compared to the orbital separation) Archimedean spiral. The peak of dust production occurs at some distance downstream from the colliding wind stagnation point.

So far, there is no direct evidence that WR 65 is a pinwheel. However, the topology and structure of circumstellar matter in a pinwheel could help to explain X-ray spectral variability in WR 65. Wilms, Allen & McCray (2000) presented a model for the absorption of X-rays that includes a treatment of dust grains. Their work confirmed that large-grain absorption for soft X-rays (<2 keV) is reduced due to the self-blanketing of grains. Interestingly, from the point of view of radiative transfer, this is identical to the reduction of opacity for the X-rays in clumped stellar winds (Feldmeier, Oskinova & Hamann 2003). Winds of WC stars are extremely rich in C and O and could have enhanced abundance of Mg and Ne. C and O are dominant absorbers for the softer X-rays (<1 keV), while Mg and Ne strongly contribute to the absorption of harder X-rays (>1 keV). In the dusty shell around a WC9d star, C would be depleted from the gaseous phase and form grains, reducing the opacity for the softer X-rays. This may help to explain the large differences between the column densities that we determine from soft and hard X-rays.

Recently, Lemaster, Stone & Gardiner (2007) presented 3D hydrodynamical simulations of colliding winds. Scaling the results of their simulation to the parameters of WR 65, soft X-ray emission could originate from a large volume extending above the orbital plane. This emission would show little variation with orbital phase and suffer comparably mild absorption in the outer regions of the WC star wind, similarly to what is observed in WR 65. On the other hand, a high post-shock temperature of $kT \approx 10$ keV is predicted for a confined region near the point where the winds collide head-on. Densities up to $\rho \gtrsim 10^{-14}$ g cm^{-3} can be expected in the dusty spiral arms. Assuming the wind opacity for hard X-rays as $\kappa \approx 5$ cm^2 g^{-1} (Antokhin, Owocki & Brown 2004), a spiral arm width of 10^{14} cm would explain the observed high absorption. This width is consistent with the observed width of the dusty spiral arms in WR 104 (Tuthill et al. 2008). The lowest absorbing column can be expected at the phase when the line of sight crosses only the outer low-density part of the spiral arms. It is possible that the *Chandra* observations of WR 65 at high state have caught this orbital phase.

To conclude, our first brief study of the variable X-ray emission from WR 65 indicates that it is a colliding wind system, where the dust and complex geometry of its colliding wind region are pivotal in explaining its X-ray properties. At present, WR 65 is the only known WC9d star where X-ray emission is detected. Future observations are needed to constrain the orbital parameters of WR 65 and allow for detailed modelling.

ACKNOWLEDGMENTS

The authors are grateful to P. M. Williams for initiating this study and to N. S. Schulz for useful discussions on the ACIS-I spectra. The authors thank the referee (A. F. J. Moffat) for detailed and helpful comments. Based on *Chandra* data: obsid 754, 6117, 6116, 5535, 5534, 5515, 4384, 3834 and 3833. This research has made use of software provided by the *Chandra* X-ray Center and data obtained through the NASA/IPAC Infrared Science Archive and High-Energy Astrophysics Science Archive Research Center. The SIMBAD data base, operated at CDS, Strasbourg, France and NASA's Astrophysics Data System were extensively used during this work.

REFERENCES

Antokhin I. I., Owocki S. P., Brown J. C., 2004, ApJ, 611, 434
Arnaud K. A., 1996, ASP Conf. Ser. Vol. 101. Astron. Soc. Pac, San Francisco, p. 17
Chapman J. M. et al., 1999, ApJ, 518, 890
Corcoran M. F. et al., 2005, in Sjouwerman L. O., Dyer K. K., eds, X-Ray and Radio Connections. NRAO (http://www.aoc.nrao.edu/events/xraydio)
DeLaney T. et al., 2006, ApJ, 640, 929
Ignace R., Oskinova L. M., Brown J. C., 2003, A&A, 408, 353
Eichler D., Usov V., 1993, ApJ, 402, 271
Feldmeier A., Oskinova L., Hamann W.-R., 2003, A&A, 403, 217
Gaensler B. M. et al., 2002, ApJ, 569, 878
Giacani E., Dubner G., 2004, A&A, 413, 225
Hamaguchi K. et al., 2007, ApJ, 663, 522
Hamann W.-R., Gräfener G., 2003, A&A, 410, 993.
Leitherer C., Chapman J. M., Koribalski B., 1997, ApJ, 481, 898
Lemaster M. N., Stone J. M., Gardiner T. A., 2007, ApJ, 662, 582
Maeda Y., Koyama K., Yokogawa J., Skinner S., 1999, ApJ, 510, 967
Marchenko S. V., Moffat A. F. J., 2007, ASP Conf. Ser. Vol. 367. Astron. Soc. Pac., San Francisco, p. 213
Marston A. P., 1997, ApJ, 475, 188
Monnier J. D., 2002, ApJ, 566, 399
Oskinova L. M., 2005, MNRAS, 361, 679
Oskinova L. M., Clarke D., Pollock A. M. T., 2001, A&A, 378, L21
Oskinova L. M. et al., 2003, A&A, 402, 755
Pittard J. M., 2007, ApJ, 660, L141
Pittard J. M. et al., 1998, MNRAS, 299, L5
Pollock A. M. T. et al., 2005, ApJ, 629, 482
Raassen A. J. J. et al., 2003, A&A, 402, 653
Rauw G., 2000, MNRAS, 316, 129
Schild H. et al., 2004, A&A, 422, 177
Smith R. K. et al., 2001, ApJ, 556, L91
Stevens I. R., Blondin J. M., Pollock A. M. T., 1992, ApJ, 386, 265
Turner D. G., 1996, AJ, 111, 828
Tuthill P. G. et al., 2008, ApJ, 675, 698
van der Hucht K. A., 2001, New Astron. Rev., 45, 135
Wallace D. J., 2007, ASP Conf. Ser. Vol. 367. Astron. Soc. Pac., San Francisco, p. 37
Williams P. M., van der Hucht K. A., Thé P. S., 1987, A&A, 182, 91
Williams P. M. et al., 1990, MNRAS, 243, 662
Willis A. J., Schild H., Stevens I. R., 1995, A&A, 298, 549
Wilms J., Allen A., McCray R., 2000, ApJ, 542, 924
Yatsu Y. et al., 2005, ApJ, 631, 312
Zhekov S. A., 2007, MNRAS, 382, 886
Zubko V. G., 1998, MNRAS, 295, 109

This paper has been typeset from a TEX/LATEX file prepared by the author.